



## NRC Publications Archive Archives des publications du CNRC

### **BN pegasi: a semidetached eclipsing binary** Nelson, Robert H.

This publication could be one of several versions: author's original, accepted manuscript or the publisher's version. / La version de cette publication peut être l'une des suivantes : la version prépublication de l'auteur, la version acceptée du manuscrit ou la version de l'éditeur.  
For the publisher's version, please access the DOI link below. / Pour consulter la version de l'éditeur, utilisez le lien DOI ci-dessous.

#### **Publisher's version / Version de l'éditeur:**

<https://doi.org/10.22444/IBVS.6201>

*Information Bulletin on Variable Stars, 6201, 2017-03-17*

#### **NRC Publications Record / Notice d'Archives des publications de CNRC:**

<https://nrc-publications.canada.ca/eng/view/object/?id=8258d597-3001-41e8-9942-a7d471609a63>;

<https://publications-cnrc.canada.ca/fra/voir/objet/?id=8258d597-3001-41e8-9942-a7d471609a63>

Access and use of this website and the material on it are subject to the Terms and Conditions set forth at

<https://nrc-publications.canada.ca/eng/copyright>

READ THESE TERMS AND CONDITIONS CAREFULLY BEFORE USING THIS WEBSITE.

L'accès à ce site Web et l'utilisation de son contenu sont assujettis aux conditions présentées dans le site

<https://publications-cnrc.canada.ca/fra/droits>

LISEZ CES CONDITIONS ATTENTIVEMENT AVANT D'UTILISER CE SITE WEB.

**Questions?** Contact the NRC Publications Archive team at

PublicationsArchive-ArchivesPublications@nrc-cnrc.gc.ca. If you wish to email the authors directly, please see the first page of the publication for their contact information.

**Vous avez des questions?** Nous pouvons vous aider. Pour communiquer directement avec un auteur, consultez la première page de la revue dans laquelle son article a été publié afin de trouver ses coordonnées. Si vous n'arrivez pas à les repérer, communiquez avec nous à PublicationsArchive-ArchivesPublications@nrc-cnrc.gc.ca.



## BN PEGASI – A SEMIDETACHED ECLIPSING BINARY

NELSON, ROBERT H.<sup>1,2</sup>

<sup>1</sup> 1393 Garvin Street, Prince George, BC, Canada, V2M 3Z1, email: bob.nelson@shaw.ca

<sup>2</sup> Guest investigator, Dominion Astrophysical Observatory, Herzberg Institute of Astrophysics, National Research Council of Canada

The variability of BN Peg (AN 145.1935; NSVS 14426159; TYC 537-44-1), amongst many others, was discovered photographically by Hoffmeister (1935) who gave coordinates, a magnitude range, and a finder chart, and described the system as an Algol. Jensch (1935) supplied elements (epoch, period) and 15 photographic eclipse timings. Mallama (1980) and Kreiner (2004) presented up-to-date elements. Over the years, there have been a number of eclipse timings, but no light curve analysis.

Light curve and radial velocity data have been acquired, but before any analysis, the first task was to examine the period variation. An eclipse timing difference (O-C) plot using all available data is reproduced in Figs. 1 and 2.

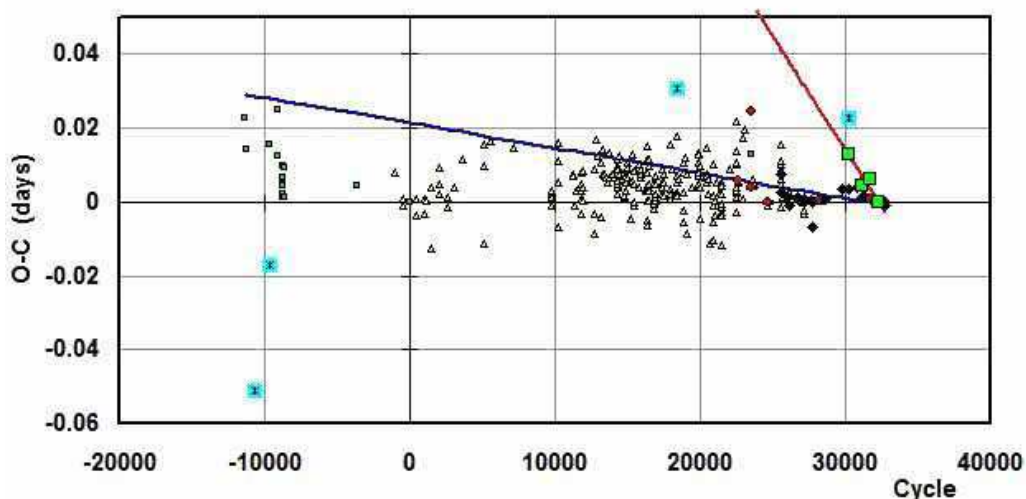


**Figure 1.** BN Peg – eclipse timing (O-C) diagram with fits to primary and secondary eclipse timings. Legend: small squares – photographic; triangles – visual; filled circles – photoelectric; filled diamonds – CCD. The four large squares are secondary minima (PE and CCD). The asterisk symbols are rejected readings.

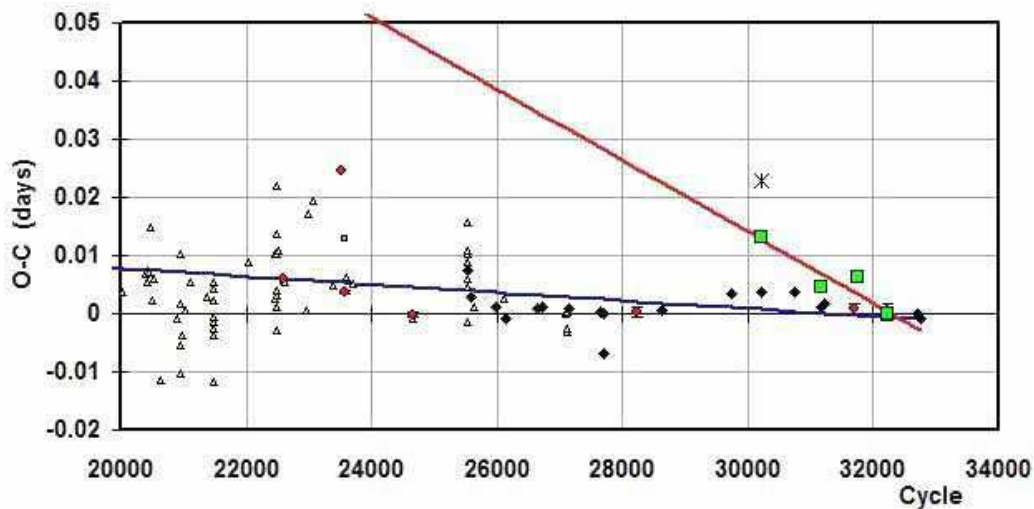


**Figure 2.** BN Peg – eclipse timing (O-C) diagram, identical to Fig. 9 but in more detail.

It will be seen that the many points since the first (in 1929) display considerable scatter. While the scatter is understandable for the photographic and visual points display, it is not clear why the photoelectric (PE) and CCD points are not more consistent. One possibility is that the system is undergoing an elliptical orbit with apsidal motion due to a third body. If that is the case, some of the supposedly deviant points would fit together with the other secondary minima to obey a different relation – that depicted in more detail in Fig. 10. (The first secondary minimum may still be deviant, however, and was not included in the fit of Fig. 10.) Also, the period may be changing over the long term, and there may even be a short-term cyclic component. However, all this is very speculative; future eclipse timings will be required to settle the matter. The eclipse timing (O-C) Excel file may be found online at Nelson (2016).

Although both the spectroscopic and photometric data were taken at about cycle 32 000, it seemed the safest procedure (in view of the scatter) to take the best-fit for the primary eclipse data from cycle 25,500 to the present. Small errors in the slope should not affect the phasing significantly. The result, equation (1) was used for all phasing.

$$\text{JD(Hel) MinI} = 2457254.7346 + 0.7132973E \quad (1)$$

In July-August of 2015, the author took 145 frames in  $V$ , 146 in  $R_C$  (Cousins) and 161 in the  $I_C$  (Cousins) band at his private observatory in Prince George, BC, Canada. The telescope was a 33 cm f/4.5 Newtonian on a Paramount ME mount; the camera was a SBIG ST-10XME. Standard reductions were then applied. The variable, comparison and check stars are listed in Table 1. The coordinates and magnitudes for all three stars are from the Tycho Catalogue (Hog et al. 2000).

In October of 2015 and again in September of 2016, the author then took a total of 9 medium resolution ( $R \sim 10000$  on average) spectra of BN Peg at the Dominion Astrophysical Observatory (DAO) in Victoria, British Columbia, Canada using the Cassegrain spectrograph attached to the 1.85 m Plaskett Telescope. He used the 21181 grating with 1800 lines/mm, blazed at  $5000 \text{ \AA}$  giving a reciprocal linear dispersion of  $10 \text{ \AA/mm}$  in the first order. The wavelengths ranged from  $5000$  to  $5260 \text{ \AA}$ , approximately. A log of observations is given in Table 2. The following elements were used for both RV and

Table 1: Details of variable, comparison and check stars.

| Object     | GSC       | RA (J2000)  | Dec (J2000)  | $V$ (mag) | $B - V$ (mag) |
|------------|-----------|---|--------------|-----------|---------------|
| Variable   | 0537-0044 | 21 <sup>h</sup> 28 <sup>m</sup> 04 <sup>s</sup> .27 | 04°59′01″.97 | 10.84(7)  | +0.43(10)     |
| Comparison | 0537-1042 | 21 <sup>h</sup> 28 <sup>m</sup> 32 <sup>s</sup> .20 | 04°57′53″.99 | 10.55(6)  | +0.97(11)     |
| Check      | 0537-0899 | 21 <sup>h</sup> 29 <sup>m</sup> 00 <sup>s</sup> .79 | 05°00′57″.50 | 10.59(6)  | +0.70(10)     |

Table 2: Log of DAO observations.

| DAO<br>Image # | Mid Time<br>(HJD−2400000) | Exposure<br>(sec) | Phase at<br>Mid-exp | $V_1$<br>(km/s) | $V_2$<br>(km/s) |
|----------------|---------------------------|-------------------|---------------------|-----------------|-----------------|
| 13241          | 57298.7895                | 3600              | 0.762               | +75.3           | −242.1          |
| 13280          | 57299.8133                | 2400              | 0.198               | −114.7          | +168.1          |
| 13318          | 57300.6283                | 2400              | 0.340               | −99.4           | +157.9          |
| 9241           | 57644.7374                | 1800              | 0.760               | +75.4           | −222.7          |
| 9308           | 57645.8432                | 360               | 0.311               | −117.5          | —               |
| 9362           | 57646.8286                | 1800              | 0.692               | +67.7           | −213.0          |
| 9445           | 57650.7527                | 1384              | 0.194               | −118.0          | +179.7          |
| 9557           | 57653.6707                | 1200              | 0.284               | −126.4          | +169.3          |
| 9559           | 57653.6860                | 1200              | 0.306               | −109.3          | +181.0          |

photometric phasing:

Frame reduction was performed by software ‘RaVeRe’ (Nelson 2009). See Nelson et al. (2014) for further details.

Radial velocities were determined using the Rucinski broadening functions (Rucinski 2004; Nelson 2010b; Nelson et al. 2014). An Excel worksheet with built-in macros (written by him) was used to do the necessary radial velocity conversions to geocentric and back to heliocentric values (Nelson 2010a). The resulting RV determinations are also presented in Table 2. For the 2015 data, the results were corrected 2.2% and 1.0% up, respectively, to allow for the small phase smearing. (Because of the shorter exposure times possible with the newly-coated optics, no correction was necessary for the 2016 data.) Correction was achieved by dividing the RVs by the factor  $f = (\sin X)/X$ ; where  $X = 2\pi t/P$ , where  $t$  denotes exposure time and  $P$  denotes the orbital period. For spherical stars, this correction is exact; in other cases, it can be shown to be close enough for any deviation to fall below observational errors. The mean rms errors for  $RV_1$  and  $RV_2$  were 4.2 and 7.7 km/s, respectively, and the overall rms deviation from the (sinusoidal) curves of best fit was 6.5 km/s. The best fit yielded the values  $K_1 = 98.7(3)$  km/s,  $K_2 = 208.6(7)$  km/s and  $V_\gamma = -22.6(4)$  km/s, and thus a mass ratio  $q_{sp} = K_1/K_2 = M_2/M_1 = 0.473(2)$ .

The author used the 2003 version of the Wilson-Devinney (WD) light curve and radial velocity analysis program with Kurucz atmospheres (Wilson and Devinney 1971; Wilson 1990; Kallrath et al. 1999) as implemented in the Windows front-end software WDwint (Nelson 2009) to analyze the data. To get started, the spectral type F5 (taken from SIMBAD, no reference given; main sequence assumed) was adopted. Interpolated tables from Cox (2000) gave a temperature  $T_1 = 6650 \pm 300$  K and  $\log g = 4.355 \pm 0.020$ . (The quoted errors refer to two and one half spectral sub-classes.) An interpolation program by Terrell (1994, available from Nelson 2009) gave the Van Hamme (1993) limb darkening values; and finally, a logarithmic (LD=2) law for the limb darkening coefficients was se-

Table 3: Limb darkening values from Van Hamme (1993) for  $T_1 = 6650$  K and  $T_2 = 4221$  K.

| Band  | $x_1$ | $x_2$ | $y_1$ | $y_2$ |
|-------|-------|-------|-------|-------|
| Bol   | 0.640 | 0.548 | 0.243 | 0.266 |
| V     | 0.705 | 0.781 | 0.280 | 0.260 |
| $R_C$ | 0.632 | 0.749 | 0.287 | 0.297 |
| $I_C$ | 0.548 | 0.664 | 0.275 | 0.309 |

lected, appropriate for temperatures  $< 8500$  K (ibid.). The limb darkening coefficients are listed below in Table 3. (The values for the second star are based on the later-determined temperature of 4248 K and assumed spectral type of K6.) Convective envelopes for both stars were used, appropriate for cooler stars (hence values gravity exponent  $g = 0.32$  and albedo  $A = 0.500$  were used for each).

From the GCVS 4 designation (EW) and from the shape of the light curve, mode 2 (detached) was used. Early on, it was noted that the maxima between eclipses were unequal. This is the O’Connell effect (Davidge & Milone 1984, and references therein) and is usually explained by the presence of one or more star spots. Because Max II (phase 0.75) was lower than Max I (phase 0.25), a solution was first obtained with a spot added to star 1. (Later on, a solution was sought with the spot on star 2 but it gave poorer residuals than the one for star 1, so the former was adopted.)

Convergence by the method of multiple subsets was reached after a considerable number of iterations. (The subsets were:  $(a, e, L_1)$ ,  $(\omega, T_2, q)$ ,  $(V_\gamma, \Omega_2)$ . and  $(e, i, \Omega_1)$ . The spots were handled separately.)

Detailed reflections were tried, with  $nref = 2$ , but there was little—if any—difference in the fit from the simple treatment. There are certain uncertainties in the process (see Csizmadia et al. 2013; Kurucz 2002). On the other hand, the solution is very weakly dependent on the exact values used.

In the first set of iterations when the fit was near, the sigmas for each dataset were adjusted, based on the output of WD (viz. computed from the sum of residuals for each dataset plus number of points). To aid in comparison between different solutions, the same sigmas were then used throughout the different trails.

Despite multiple trials, no completely satisfactory solution could be reached in mode 2 with  $T_1 = 6650$  K. (The fit for the secondary eclipse in the  $I$  band was poor.) A better solution was achieved by assuming an earlier spectral type, that of F2, with a temperature of  $T_1 = 7000$  K (Cox 2000). Designate these as solutions A and B, respectively. Additional considerations (see later discussion) suggested that mode 5 (Algol) should be investigated. Trials therefore were made with mode 5 at the same two temperatures. Solution D with  $T_1 = 7000$  K was unsatisfactory, but solution C with  $T_1 = 6650$  K stood out from all the rest for a number of reasons to be discussed later.

All four models are presented in Table 4. Note that estimating the uncertainties in temperatures  $T_1$  and  $T_2$  is somewhat problematic. A common practice is to quote the temperature difference over—say—1.5 spectral sub-classes (assuming that the classification is good to one spectral sub-classes, the precision being unknown). In addition, various different calibrations have been made (Cox 2000, pages 388-390 and references therein, and Flower 1996), and the variations between the various calibrations can be significant. (Flower gives  $T_1 = 6542$  K for F5 for example.) However, there is an additional uncertainty here because a spectral type (for star 1) is assumed to be F2. Therefore, a larger uncertainty, that of two and one half spectral sub-classes is adopted here, giving

an uncertainty of  $\pm 300$  K to the absolute temperatures of each. The modelling error in temperature  $T_2$ , relative to  $T_1$ , is indicated by the WD output to be much smaller, around 20 K.

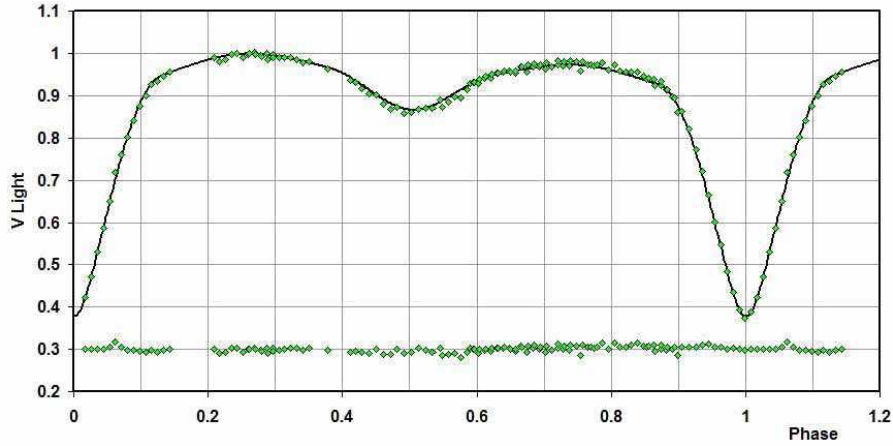


**Figure 3.** *V* light curves for BN Peg (solution C) – data, WD fit, and residuals.

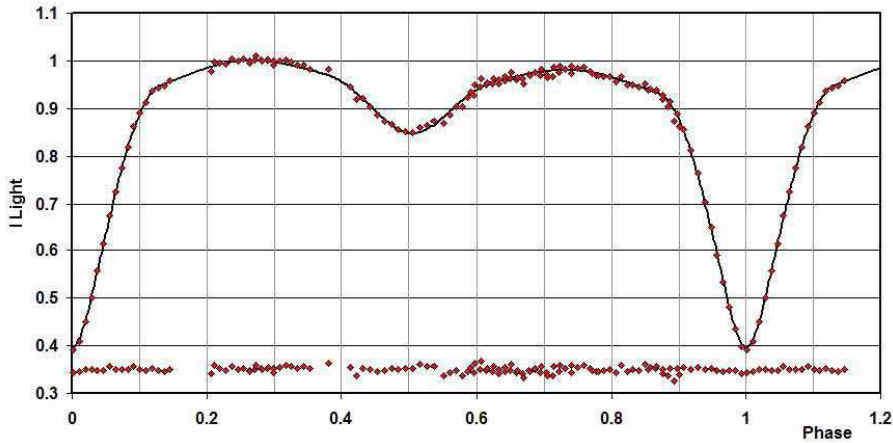


**Figure 4.** *R* light curves for BN Peg (solution C) – data, WD fit, and residuals.

The light curve data and the fitted curves for solution C are depicted in Figures 3–5. The residuals (in the sense observed-calculated) are also plotted, shifted upwards by 0.30, 0.35, and 0.35 units, respectively.

The radial velocities and the fit of solution C are shown in Fig. 6. A three-dimensional representation from Binary Maker 3 (Bradstreet 1993) is shown in Fig. 7.

The WD output fundamental parameters and errors are listed in Table 5. Most of the errors are output or derived estimates from the WD routines. From Kallrath & Milone (1999), the fill-out factor is  $f = (\Omega_I - \Omega)/(\Omega_I - \Omega_O)$ , where  $\Omega$  is the modified Kopal potential of the system,  $\Omega_I$  is that of the inner Lagrangian surface, and  $\Omega_O$ , that of the outer Lagrangian surface, was also calculated.

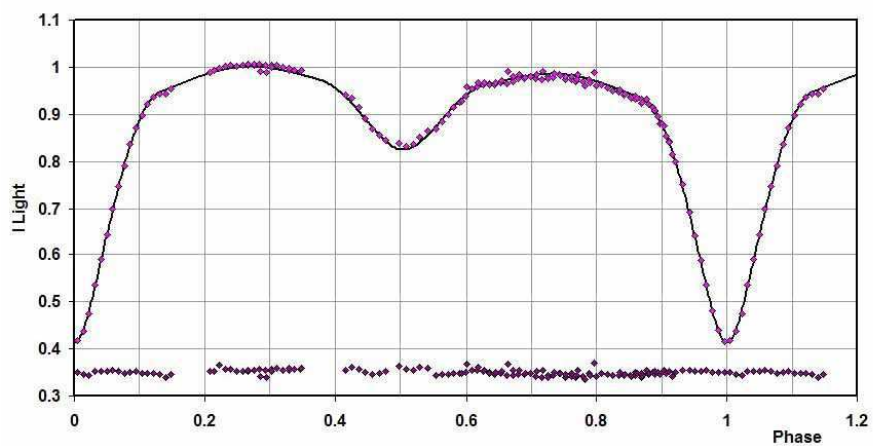


Figure 5. *I* light curves for BN Peg (solution C) – data, WD fit, and residuals.

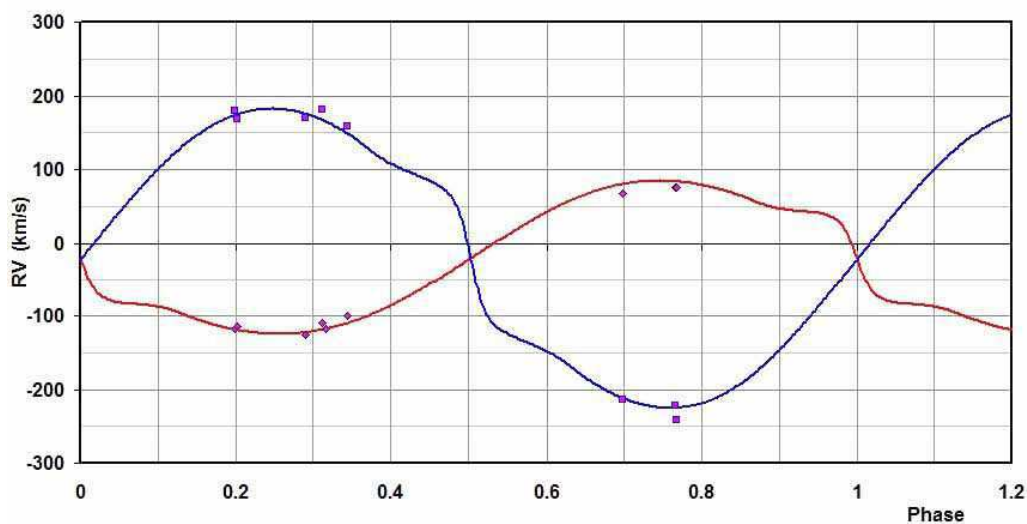


Figure 6. Radial velocity curves for BN Peg – data and WD fit.



Figure 7. Binary Maker 3 representation of the system – at phases 0.75 and 0.97.

Table 4: Wilson-Devinney parameters.

| Solution >>                 | A       | B       | C       | D       |         |           |
|-----------------------------|---------|---------|---------|---------|---------|-----------|
| WD Quantity                 | value   | value   | value   | value   | error   | unit      |
| Mode                        | 2       | 2       | 5       | 5       | —       | —         |
| Spectral type               | F5      | F2      | F5      | F2      | —       | —         |
| Temperature $T_1$           | 6650    | 7000    | 6650    | 7000    | [fixed] | K         |
| Temperature $T_2$           | 4248    | 4388    | 4221    | 4389    | 20      | K         |
| $q = m_2/m_1$               | 0.490   | 0.505   | 0.486   | 0.505   | 0.004   | —         |
| Potential $\Omega_1$        | 3.108   | 3.133   | 3.159   | 3.175   | 0.008   | —         |
| Potential $\Omega_2$        | 2.901   | 2.944   | 2.881   | 2.903   | 0.008   | —         |
| Inclination, $i$            | 83.4    | 83.5    | 82.6    | 82.2    | 0.1     | deg       |
| Semi-maj. axis, $a$         | 4.59    | 4.61    | 4.59    | 4.61    | 0.06    | sol. rad. |
| Syst. velocity, $V_\gamma$  | -22.0   | -20.8   | -20.8   | -20.8   | 1.8     | km/s      |
| Eccentricity, $e$           | 0.006   | 0.006   | 0.014   | 0.008   | 0.001   | —         |
| Phase shift                 | 0.0028  | 0.0028  | 0.0023  | 0.0025  | 0.0003  | —         |
| Arg. periastron, $\omega$   | 19.2    | 19.1    | 17.6    | 19.8    | 0.1     | deg       |
| Spot co-latitude            | 81      | 75      | 79      | 75      | 10      | deg       |
| Spot longitude              | 74      | 78      | 81      | 78      | 5       | deg       |
| Spot radius                 | 27.4    | 27.4    | 34.9    | 27.4    | 4       | deg       |
| Spot temp. factor           | 0.9659  | 0.9650  | 0.9793  | 0.9650  | 0.0020  | —         |
| $L_1/(L_1 + L_2)$ ( $V$ )   | 0.9475  | 0.9472  | 0.9460  | 0.9417  | 0.0002  | —         |
| $L_1/(L_1 + L_2)$ ( $R_C$ ) | 0.9222  | 0.9243  | 0.9195  | 0.9169  | 0.0003  | —         |
| $L_1/(L_1 + L_2)$ ( $I_C$ ) | 0.8952  | 0.8991  | 0.8911  | 0.8897  | 0.0004  | —         |
| $r_1$ (pole)                | 0.3777  | 0.3762  | 0.3707  | 0.3707  | 0.0004  | orb. rad. |
| $r_1$ (point)               | 0.4329  | 0.4320  | 0.4205  | 0.4216  | 0.0008  | orb. rad. |
| $r_1$ (side)                | 0.3946  | 0.3930  | 0.3862  | 0.3864  | 0.0005  | orb. rad. |
| $r_1$ (back)                | 0.4116  | 0.4103  | 0.4020  | 0.4026  | 0.0006  | orb. rad. |
| $r_2$ (pole)                | 0.2914  | 0.2917  | 0.2944  | 0.2987  | 0.0003  | orb. rad. |
| $r_2$ (point)               | 0.3756  | 0.3695  | 0.4216  | 0.4274  | 0.0017  | orb. rad. |
| $r_2$ (side)                | 0.3032  | 0.3033  | 0.3068  | 0.3115  | 0.0003  | orb. rad. |
| $r_2$ (back)                | 0.3324  | 0.3313  | 0.3389  | 0.3438  | 0.0005  | orb. rad. |
| $\sum \omega_{res}^2$       | 0.01801 | 0.01745 | 0.01737 | 0.01845 | —       | —         |

Table 5: Fundamental parameters.

| Solution >>>       | A     | B      | C     | D     | Error | unit      |
|--------------------|-------|--------|-------|-------|-------|-----------|
| Quantity           | value | value  | value | value |       |           |
| mode               | 2     | 2      | 5     | 5     | —     | —         |
| Temperature, $T_1$ | 6650  | 7000   | 6650  | 7000  | 300   | K         |
| Temperature, $T_2$ | 4248  | 4338   | 4221  | 4389  | 300   | K         |
| Mass, $m_1$        | 1.717 | 1.723  | 1.725 | 1.723 | 0.05  | $M_\odot$ |
| Mass, $m_2$        | 0.841 | 0.870  | 0.839 | 0.870 | 0.004 | $M_\odot$ |
| Radius, $R_1$      | 1.81  | 1.82   | 1.78  | 1.78  | 0.02  | $R_\odot$ |
| Radius, $R_2$      | 1.42  | 1.43   | 1.45  | 1.47  | 0.02  | $R_\odot$ |
| $M_{bol,1}$        | 2.88  | 2.66   | 2.93  | 2.70  | 0.1   | mag       |
| $M_{bol,2}$        | 5.36  | 5.21   | 5.35  | 5.14  | 0.1   | mag       |
| Log $g_1$          | 4.16  | 4.16   | 4.18  | 4.17  | 0.01  | cgs       |
| Log $g_2$          | 4.06  | 4.07   | 4.04  | 4.04  | 0.02  | cgs       |
| Luminosity, $L_1$  | 5.8   | 7.1    | 5.5   | 6.9   | 0.5   | $L_\odot$ |
| Luminosity, $L_2$  | 0.59  | 0.68   | 0.60  | 0.72  | 0.05  | $L_\odot$ |
| Fill-out factor 1  | -0.86 | -0.822 | -1.06 | -0.96 | 0.10  | —         |
| Fill-out factor 2  | -0.15 | -0.20  | 0     | 0     | 0.10  | —         |
| Distance, $r$      | 354   | 394    | 345   | 389   | 35    | pc        |

To determine the distance  $r$ , the analysis (using solution C) proceeded as follows: First the WD routine gave the absolute bolometric magnitudes of each component; these were then converted to the absolute visual ( $V$ ) magnitudes of both,  $M_{V,1}$  and  $M_{V,2}$ , using the bolometric corrections  $BC = -0.140$  and  $-0.984$  for stars 1 and 2 respectively. The latter were taken from interpolated tables constructed from Cox (2000). The absolute  $V$  magnitude was then computed in the usual way, getting  $M_V = 3.02 \pm 0.20$  magnitudes. The apparent magnitude in the  $V$  passband was  $V = 10.84 \pm 0.07$ , taken from the Tycho values (Hog et al. 2000) and converted to a Johnson magnitude using relations due to Henden (2001). The colour excess (in  $B - V$ ) was obtained in the usual way, by subtracting the tabular value of  $B - V$  (for that spectral class) from the observed (converted Tycho) value. This gave  $E[B - V] = -0.07$  magnitudes which is not physically possible. However, reference to the dust tables of Schlegel et al. (1998) revealed a value of  $E[B - V] = 0.063$  for those galactic coordinates. Since the  $E[B - V]$  values have been derived from full-sky far-infrared measurements, they therefore apply to objects outside of the Galaxy; this value of  $E[B - V]$  so derived then represents an upper limit for closer objects within the Galaxy. Hence the lower value of half that, 0.032 is reasonable, and was adopted. (An uncertainty of—say—half this amount was used in the error calculation for distance.)

Galactic extinction was obtained from the usual relation  $A_V = R E[B - V]$ , using  $R = 3.1$  for the reddening coefficient. Hence, for solution C, a distance  $r = 345$  pc was calculated from the standard relation:

$$r = 10^{0.2(V - M_V - A_V + 5)} \text{ pc} \quad (2)$$

The errors were assigned as follows:  $\delta M_{bol,1} = \delta M_{bol,2} = 0.01$ ,  $\delta BC_1 = 0.020$ ,  $\delta BC_2 = 0.330$  (the variation of 2.5 spectral sub-classes),  $\delta V = 0.07$ ,  $\delta E(B - V) = 0.10$ , all in magnitudes, and  $\delta R = 0.1$ . Combining the errors rigorously (i.e., by adding the variances) yielded an estimated error in  $r$  of 35 pc.

The evolutionary status of this system is interesting. Solution A (detached, F5,  $T_1$

= 6650 K) gives a primary mass, radius and luminosity that are too large for the zero age main sequence (ZAMS) values listed in column 3 (Cox, 2000). Reference to the evolutionary tables of Schaller et al. (1992, solar type, mass 1.7 solar masses, their table 16) reveals that the temperature of  $T_1 = 6650$  K is too low to fit the terminal age main sequence (TAMS) or any evolved state. Solution A is therefore rejected.

Turning to solution B (detached, F2,  $T_1 = 7000$  K), one might believe that star 1 started with a higher temperature on the TAMS but cooled as it evolved. However, reference to the same evolutionary tables (ibid) reveals that, for an age of 1.3 Gy, the temperature would fit, but then the actual luminosity at  $7.1 L_\odot$  would be too small for their computed value of  $11.3 L_\odot$ . For this reason, we reject solution B.

Solution C (Algol, F5,  $T_1 = 6650$  K) fits better because temperature  $T_1$  matches the assumed spectral type, the mass ratio matches the spectrographic value, and the sum of residuals squared is the lowest of the four solutions. Also, most importantly, Solution C makes sense because Algols are known to have experienced mass flow from the secondary (but originally more massive star) to its companion. That would explain the excess mass for the F5 star. Its larger radius would then account for the higher luminosity. Therefore we adopt solution C (mode 5, Algol) as the correct one.

In conclusion, the fundamental parameters of this system have been determined, albeit to a somewhat lower level of precision than one would like. It is to be hoped that higher precision data from a planned remote site with routine photometric skies plus a renewed classification will confirm the exact nature of this system.

*Acknowledgements:* It is a pleasure to thank the staff members at the DAO (especially Dmitry Monin and David Bohlender) for their usual splendid help and assistance.

#### References:

- Bradstreet, D.H., 1993, "Binary Maker 2.0 - An Interactive Graphical Tool for Preliminary Light Curve Analysis", in Milone, E.F. (ed.) *Light Curve Modelling of Eclipsing Binary Stars*, pp 151-166 (Springer, New York, N.Y.)
- Cox, A.N. 2000, *Allen's Astrophysical Quantities*, 4th ed., (Springer, New York, NY)
- Csizmadia, S., Pasternacki, T., Dreyer, C., Cabrera, A., Erikson, A., Rauer, H., 2013, *A&A*, **549**, A9 DOI
- Davidge, T.J., Milone, E.F., 1984, *ApJS*, **55**, 571 DOI
- Flower, P.J., 1996, *ApJ*, **469**, 355 DOI
- Henden, A., 2001, <http://www.tass-survey.org/tass/catalogs/tycho.old.html>
- Hoffmeister, C. von, 1935, *AN*, **255**, 401 DOI
- Høg, E., et al., 2000, *A&A*, **355**, L27
- Jensch, A. von, 1935, *AN*, **255**, 417 DOI
- Kallrath, J., Milone, E.F., 1999, *Eclipsing Binary Stars—Modeling and Analysis* (Springer-Verlag)
- Kallrath, J., Milone, E.F., Terrell, D., Young, A.T., 1998, *ApJ*, **508**, 308 DOI
- Kreiner, J.M., 2004, *AcA*, **54**, 207
- Kurucz, R.L., 2002, *Baltic Astron.*, **11**, 101
- Mallama, A.D., 1980, *ApJS*, **44**, 241 DOI
- Nelson, R.H., 2009, Software, [http://www.variablestarssouth.org/profilegrid\\_blogs/software-by-bob-nelson/](http://www.variablestarssouth.org/profilegrid_blogs/software-by-bob-nelson/)

- Nelson, R.H., 2010a, Spreadsheets, [http://www.variablestarssouth.org/profilegrid\\_blogs/spreadsheets-by-bob-nelson/](http://www.variablestarssouth.org/profilegrid_blogs/spreadsheets-by-bob-nelson/)
- Nelson, R.H., 2010b, “Spectroscopy for Eclipsing Binary Analysis” in The Alt-Az Initiative, Telescope Mirror & Instrument Developments (Collins Foundation Press, Santa Margarita, CA), R.M. Genet, J.M. Johnson and V. Wallen (eds)
- Nelson, R.H., 2016, Bob Nelson’s *O-C* Files, <http://www.aavso.org/bob-nelsons-o-c-files>
- Nelson, R. H., Şenavcı, H.V. Baştürk, Ö., Bahar, E., 2014, *New Astron.*, **29**, 57 DOI
- Rucinski, S. M., 2004, *IAUS*, **215**, 17
- Schaller, G., Schaerer, D., Meynet, G., Maeder, A., 1992, *A&AS*, **96**, 269
- Schlegel, D.J., Finkbeiner, D.P., Davis, M., 1998, *ApJ*, **500**, 525 DOI
- Terrell, D., 1994, Van Hamme Limb Darkening Tables, vers. 1.1.
- Van Hamme, W., 1993, *AJ*, **106**, 2096 DOI
- Wilson, R.E., Devinney, E.J., 1971, *ApJ*, **166**, 605 DOI
- Wilson, R.E., 1990, *ApJ*, **356**, 613 DOI